Available online at www.dergipark.org.tr/en

INTERNATIONAL ADVANCED RESEARCHES
and
ENGINEERING JOURNAL

Journal homepage: www.dergipark.org.tr/en/pub/iarej

e-ISSN: 2618-575X

International Open Access

Volume 05
Issue 02

August, 2021

*Research Article*

# Mathematical modeling and production of semi-active hand prosthesis from clear resin

***Mehmet Kayrıcı*** [a], ***Yusuf Uzun*** [b,*], ***Onur Gök*** [c] ***and Hüseyin Arıkan*** [a]

[a]*Department of Mechanical Engineering, Faculty of Seydisehir Ahmet Cengiz Engineering, Necmettin Erbakan University, Konya 42370, Turkey*
[b]*Department of Computer Engineering, Faculty of Seydisehir Ahmet Cengiz Engineering, Necmettin Erbakan University, Konya 42370, Turkey*
[c]*Department of Machinery and Metal Technologies, Seydi³ehir Vocational School, Necmettin Erbakan University, Konya 42370, Turkey*

ARTICLE INFO

*Article history:*
Received 30 November 2020
Revised 25 February 2021
Accepted 13 April 2021

*Keywords:*
Finite element method
Hand prosthesis
Kinematic
Kinetic

ABSTRACT

In this study, the static, kinematic and dynamic behaviors of a semi-active hand prosthesis were analyzed numerically. Finite Elements method was used in static analysis and analytical method was used in kinematic and dynamic analysis. The mathematical model of the hand was created in kinematic and dynamic analysis. Using the mathematical model obtained, torque values of 0, 15, 30, 45, 60, 75, 90 degrees were calculated according to the different position angles of the fingers. Examination was performed for 4 fingers (index finger, middle finger, ring finger, little finger) and 5 kg of force was applied to the fingertips perpendicular to the finger plane. In this examination, the forces are divided into 25% for the index finger, 35% for the middle finger, 25% for the ring finger and 15% for the little finger. The results obtained for forces at different angles under the specified conditions were explained. As a result of all these stages, the prosthetic hand was designed. The design was calculated as linear statically by the finite element method. As a result of the study, a semi-active prosthetic hand was produced considering the calculation findings. Clear resin was used as material.

© 2021, Advanced Researches and Engineering Journal (IAREJ) and the Author(s).

## 1. Introduction

Biomechanics is a discipline that examines the internal and external interactions of systems designed using engineering principles [1]. Today, biomechanics has gained great importance with the development of engineering science. Thanks to the rapid developments in technology, many applications have been developed in this area. Although the limb has a complex structure, it is possible for a prosthetic hand to approach the mobility of the real hand limb with the use of developing technology [2]. Bionic limbs are vital for people with limb loss. Hand limbs are very important for the individual's sensitivity in environmental interaction. Loss of the upper limb causes physical and psychological impairment in the life of an amputated person. Studies show that 67% of upper extremity losses are male and in the fertile age range of 16-54. However, it has emerged that 35% of them do not use the prostheses they have [3]. Pouliquen et al. suggested that the problem of lack and difficulty of use caused by psychological or lack of appearance and functionality can be solved by cosmetic improvement, comprehension, and high controllability [4]. Kerpa et al. in order to realize human-robot cooperation in housework, they worked on a robot arm that can be controlled by physiological sensors and sometimes manually [5]. Butz et al. performed the stress model in the finger joints for activities such as writing on the keyboard, playing the piano, holding a pencil, carrying weight and opening a jar [6]. Undesired limb losses for any reason not only affect the minimum quality of life of people in their daily life, but also cause a great devastation in human psychology [7, 8]. The most important reason for this is that the human hand is both a sense organ and one of the most important limbs that help

* Corresponding author. Tel.: *+90-332-582-6000.*
E-mail addresses: mkayrici@erbakan.edu.tr *(M. Kayrıcı)*, yuzun@erbakan.edu.tr *(Y. Uzun)*, ogok@erbakan.edu.tr *(O. Gök)*, harikan@erbakan.edu.tr *(H. Arıkan)*
ORCID: 0000-0003-1178-5168 *(M. Kayrıcı)*, 0000-0002-7061-8784 *(Y. Uzun)*, 0000-0003-1160-1963 *(O. Gök)*, 0000-0003-1266-4982 *(H. Arıkan)*
DOI: 10.35860/iarej.833538
This article is licensed under the CC BY-NC 4.0 International License (https://creativecommons.org/licenses/by-nc/4.0/).

us meet our minimum life needs. Loss of the limb inevitably impedes the individual's freedom of movement [9]. Today, approaching the functionality of the real human hand with mechanical, cosmetic, electronic and control mechanisms will be possible with interdisciplinary studies.

A wide range of technologies should be considered when designing and developing a prosthetic hand. In the design, not only the idea of facilitating human life, but also factors such as mental health of people, ability to grasp objects well, adaptation of the material to the body, ability to act independently, movement speed and grasping should be taken into consideration [10]. Butz et al. used a two-dimensional geometry method to determine the resulting joint and tendon forces of the hand in their model designed for the analysis of finger forces. Since the static force analysis resulted in an uncertain system, the method developed by Weightman and Amis (1982) [11] was used with the assumption that force ratios at tendon junctions are scaled proportionally to cross-sectional areas [6]. It should be well known that all bone, muscle and tendon structures of the human hand add realistic features to the limb. Atasoy et al. studied the mechanical structure of the index finger [12]. The human hand has 24 degrees of freedom kinematically. The grasping movement of the hand structure is performed by tendons attached to joints and nerves that stimulate the hand muscles [13]. Prosthetic hands such as Otto Bock 6 or VASI 7-11 are devices that hold two fingers opposite a thumb. Prosthetic hands designed in this way have some limitations. Since they are limited to opening and closing movements within a single degree of freedom, they have a limited mechanical function [7]. It appears that a large number of prosthetic hands have been developed in recent years [14]. To design a good hand limb, this limb must first be modeled mathematically [15]. Despite the complexity of the human hand, it is possible to model the finger joints kinematically [16]. Cobos et al. made some studies on hand kinematics and obtained some equations as a result of these studies [17]. Ryew and Choi designed a kinematically 2 degree of freedom joint design [18]. Zhe Xu and Emanuel Todorov designed a 3D hand design at Washington University and produced a hand functionally very close to the finger limbs [19]. José Alfredo Leal-Naranjo et al. analyzed the 3-arm hand structure (thumb, index finger, middle finger) statically and dynamically using the finite element method [20]. Gregor Harih et al. examined the finger model in the 3-dimensional finite element method and as a result found the contact force of the finger limb. Recently, studies on how to use the finite element method in mechanical design in biomedical field have been started [21]. Antoanela N. et al., by examining the bone structure of the finger limb using the finite element method, concluded that using experimental and numerical studies together is effective in understanding the behavior of the limb [22].

The main purpose of this study is to model the human hand dynamically according to physical bases, to explain the system mathematically with certain variables and to produce an optimized hand model according to these findings. To achieve this, a mathematical model of a finger limb must be kinematically constructed. The static loads on the pin elements were calculated by examining the hand model with the linear static method using the finite element method and the prosthesis was designed in a healthier way. Another aim of this study is to reduce the raw material cost in manual production. Cost is a very important factor in prosthetic hand production.

## 2. Material and Method

### *2.1 Equipment and materials*

Solidworks software was used to create the CAD model of the prosthetic hand. The CAD geometry of the finger limb to be analyzed statically with this CAD program has been made as a solid design. After static analysis and finite element mathematical modeling, Cosmos Works software was used to perform linear static analysis. A Formlab Form2 3D printer model was used to produce a prosthetic hand. The technical features of the 3D printer used were shown in Table 1. The printer used was provided by 3D fab.

The thickness was chosen as 25 microns for a total production time of 12 hours. Finger models produced were invested in alcohol. In accordance with the recommendation of the resin and the printer manufacturer, the models, which were rigid with alcohol, were then cured by exposure to ultraviolet light. The CAD geometry obtained from the SolidWorks software was converted to STL format and produced with a prosthetic hand printer. Clear resin material is used as printing material. The mechanical properties of the material used were shown in Table 2. The clear resin material used was provided by the 3bfab company.

Table 1. 3D printer features used

| Attributes | Values |
|---|---|
| Dimensions | 35x33x52 cm |
| Operation Temperature | 35 °C maximum |
| Power Requirements | 100–240 V, 2A 50/60 hz, 65W |
| Laser Properties | EN 60825-1, 405nm, 250W |
| Technology | Stereolithography (SLA) |
| Print Area | 14.5 × 14.5 × 17.5 cm |
| Layer Thickness | 25, 50, 100, 200 microns |

Table 2. Mechanical properties of celar resin used

| Attributes | Values |
|---|---|
| Type of material | Clear resin |
| Tensile Strength | 65 MPa |
| Young's Modulus | 2.8 GPa |
| Heat Deflection Temperature | 0.45 MPa, 289 °C |

The material used in the tendon design was supplied from the UK Open Bionics company. Mechanical properties of the material were given in Table 3.

The spring material and mechanical properties placed on the joints to provide the opening mechanism of the hand mechanism were shown in Table 4. These springs were supplied by Sakarya Yay Mak.

A total of 5 linear motors were used for the finger controls of the prosthetic hand. Motor selections were provided by Open Bionics company based on dynamic calculation results. The mechanical properties of the supplied motors were given in Table 5.

Schematic representation of the materials used in the prosthesis was shown in Figure 1. The hand prosthesis, which grips with the motion of tendon and linear motors, was opened with the tension force of the springs.

### *2.2 Kinematic and dynamic analysis*

The human hand anatomically has 8 carpal bones, 5 metacarpal bones and 14 phalanges bones [22]. There are 14 joints that connect the phalanges bone group and provide the planar movement of the fingers. These joints are marked in red in Figure 2.

In this study, the mathematical model of the index, middle, ring and little finger in kinematic and dynamic terms is obtained by assuming that the motion is planar. Kinematic and dynamic mathematical modeling was done by analytical method.

Table 3. Mechanical properties of tendon material

| Attributes | Values |
|---|---|
| Maximum tensile load | 45.35 kg |
| Tendon diameter | 0.75 mm |

Table 4. Mechanical properties of spring material

| Attributes | Values |
|---|---|
| Type of material | Stainless Steel |
| Spring Diameter | 0.9 mm |
| Winding Number | 6 |
| Spring inner diameter | 2.1 mm |
| Spring span | 180 degrees |
| k stiffness value | 163 N / mm |

Table 5. Mechanical properties of motors.

| Attributes | Values |
|---|---|
| Gearing Option | 63:1 |
| Peak Power Point | 30 N; 8 mm/s |
| Peak Efficiency Point | 12 N; 12 mm/s |
| Max Speed (no load) | 15 mm/s |
| Max Force (lifted) | 45 N |
| Max Side Load | 10 N |
| Back Drive Load | 25 N |
| Stroke | 20 mm |

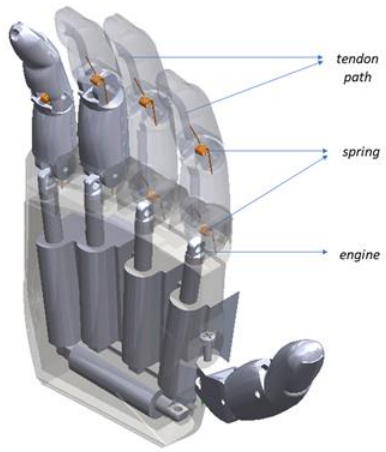


Figure 1. Schematic representation of the materials used on the prosthesis

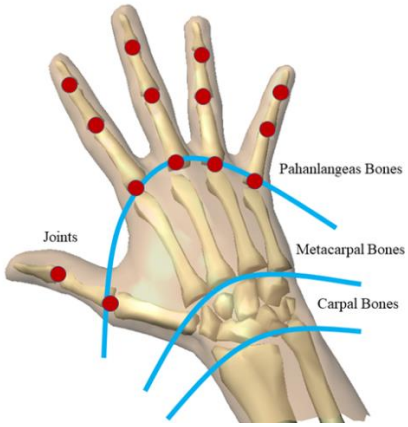


Figure 2. Anatomical hand structure [15]

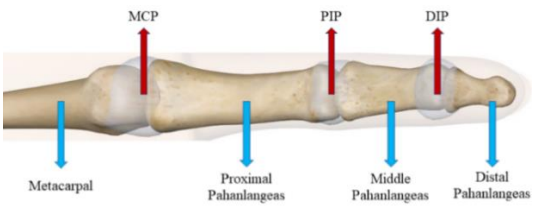


Figure 3. Anatomical finger structure [26]

There are 3 joints in the bones of the phalanges group in human anatomy (except the thumb). As shown in Figure 3, these are the MCP joint connecting the metacarpal to the proximal phalangeal, the PIP joint connecting the proximal phalangeal to the middle phalangeal, and the DIP joint connecting the middle phalanges to the distal phalanges [24, 25].

In the study, kinematic equations of a finger were obtained first and the working range was determined. To create the kinematic model of the hand, the equations of motion of the finger model must be obtained. Finger anatomy consists of cylindrical and spherical structures. DIP, PIP and MCP connections can be thought of as a single degree of freedom rotary connection. The assumptions made on the finger model in the kinematic analysis were shown in Figure 4.

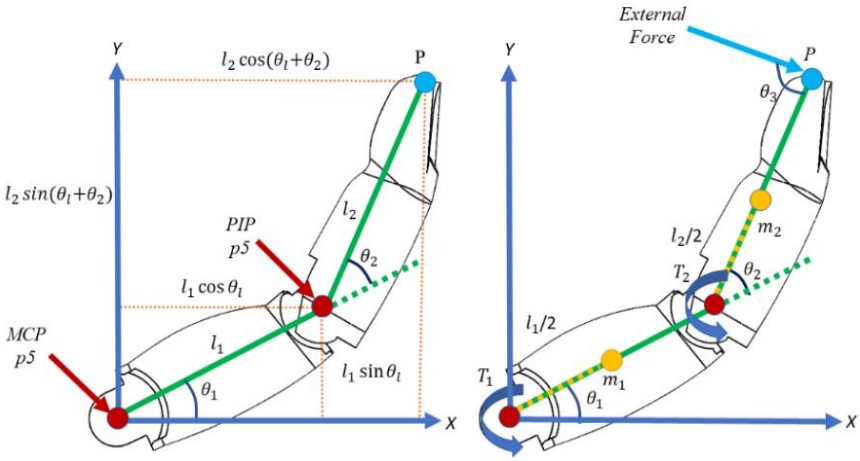


Figure 4. Kinematic and dynamic finger model

In the finger model in the figure, the MCP joint was accepted at the origin point, while the DIP joint was accepted as the fixed limb. Where, $l_1$ and $l_2$ are the lengths of the finger limbs of the kinematic finger model. The *P* denotes the position at the end point of the kinematic finger model. In space, an object has six degrees of freedom. If the degree of freedom in space was expressed by the formula, it is possible to express it as shown in Equation (1).

$$W = 6n - 5p5 - 4p4 - 3p3 \tag{1}$$

In Equation (1), *W* represents the degree of freedom, n is the number of mobile limbs, *p5* is one degree of freedom, *p4* is two degrees of freedom, and *p3* is three degrees of freedom, the moving limbs. The two-dimensional degree of freedom in the plane is as expressed in Equation (2).

$$W = 3n - 2p5 - p4 \tag{2}$$

The finger model in Figure 4 is a two degree of freedom mechanism. In Equation (3), Denavit-Hartenberg method was used to express *P* position kinematically. For the two-limb finger model in Figure 4, this equation can be written as Equation (A1) in Appendix. In the three-jointed finger model, the transformation matrices for all joints can be extracted as specified in Appendix with Equations (A2), (A3), (A4).

$${}^{0}_{N}T = {}^{0}_{1}T\,{}^{1}_{2}T\,{}^{2}_{3}T \ldots {}^{N-1}_{N}T \tag{3}$$

From these equations, $P_X$ and $P_y$ positions specified in Equation (4) was obtained.

$$\begin{aligned} P_X &= l_1 cos\theta_1 + l_2 cos\,(\theta_1+\theta_2) \\ P_y &= l_1 sin\theta_1 + l_2 sin\,(\theta_1+\theta_2) \end{aligned} \tag{4}$$

For dynamic analysis modeling boundary conditions, internal and external forces were determined. Internal forces are masses of the finger limb. External force is the $F_{external}$ force applied separately for each finger limb. These boundary conditions were given in Table 6.

Table 6. Finger physical sizes

| Fingers | $m_1$ | $m_2$ | $F_{external}$ | $l_1$ | $l_2$ |
|---|---|---|---|---|---|
| Index finger | 0.005 | 0.004 | 12.5N | 0.037m | 0.040m |
| Middle finger | 0.006 | 0.005 | 17.5N | 0.042m | 0.046m |
| Ring Finger | 0.006 | 0.004 | 12.5N | 0.039m | 0.033m |
| Little finger | 0.003 | 0.003 | 7.5N | 0.040m | 0.035m |

For the dynamic analysis, the mass center positions of the finger limbs were found with Equations (5) and (6). Afterwards, the speeds of these positions for the kinetic energy calculation were found by Equation (7) and (8).

$$\begin{bmatrix} x_1 \\ y_1 \end{bmatrix} = \begin{bmatrix} \frac{l_1}{2} cos\theta_1 \\ \frac{l_1}{2} sin\theta_1 \end{bmatrix} \tag{5}$$

$$\begin{bmatrix} x_2 \\ y_2 \end{bmatrix} = \begin{bmatrix} l_1 cos\theta_1 + \frac{l_2}{2} cos\,(\theta_1+\theta_2) \\ l_1 sin\theta_1 + \frac{l_2}{2} sin\,(\theta_1+\theta_2) \end{bmatrix} \tag{6}$$

$$\begin{bmatrix} \dot{x}_1 \\ \dot{y}_1 \end{bmatrix} = \begin{bmatrix} -\frac{l_1}{2} sin\,\theta_1\,\dot{\theta}_1 \\ \frac{l_1}{2} cos\,\theta_1\,\dot{\theta}_1 \end{bmatrix} \tag{7}$$

$$\begin{bmatrix} \dot{x}_2 \\ \dot{y}_2 \end{bmatrix} = \begin{bmatrix} -l_1 sin\,\theta_1\,\dot{\theta}_1 - \frac{l_2}{2}(\dot{\theta}_1+\dot{\theta}_2) sin\,(\theta_1+\theta_2) \\ l_1\,cos\,\theta_1\,\dot{\theta}_1 + \frac{l_2}{2}(\dot{\theta}_1+\dot{\theta}_2) cos\,(\theta_1+\theta_2) \end{bmatrix} \tag{8}$$

After these calculations, the total kinetic energy formula Equation (A5) was obtained. After calculating potential energy with Equation (A6), $T_{internal1}$ and $T_{internal2}$ equation sets specified in Equations (A8) and (A9) for the finger limb under the influence of internal forces were found by using the Lagrange equation specified by Equation (A7). Finally, the torque values under the influence of internal and external forces were obtained using $T_{total1}$ and $T_{total2}$ Equation (A10).

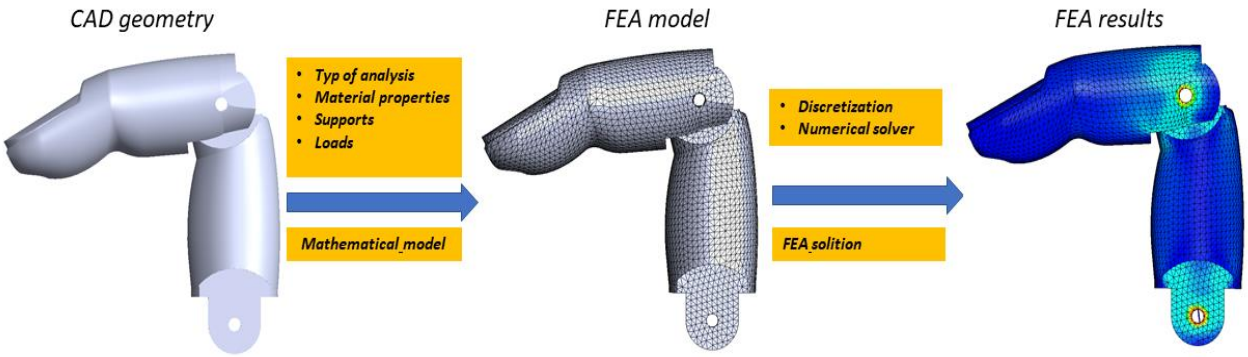


Figure 5. Static analysis processes

With these mathematical equations obtained, torque values for different angle positions (for 0, 15, 30, 45, 60, 75 degrees) were calculated separately for the index, middle, ring and little finger.

### *2.2 Static analysis*

After kinematic and dynamic analysis, finger limb was statically analyzed by finite element method. Solidworks simulation finite element package program was used for this study. Analysis modeling was done with linear static analysis acceptance. It is assumed that displacement against the load is linear.

This is because the part up to plastic deformation is to be examined. It is important for the stress values and distribution in the structure of the finger limb that remains under force. Firstly, CAD geometry was created for static analysis. A mathematical model was created from the CAD geometry created afterwards. Resin material, linear elastic isotropically, the mechanical properties of the material were introduced to the package program, and the degree of freedom limitations and forces were applied. After these steps, the analysis was run and the results shown in Figure 5 were obtained.

For degree of freedom limitations, zero degrees of freedom are defined on the hinge surfaces at the bottom of the finger model and these surfaces are built-in support. 1.25 kg load is made and shown as a force perpendicular to the finger surface. In Figure 6, the Tet element is used as the mathematical model. The mathematical model used is 10 nodes for each element. In the Solidworks simulation program, the most sensitive solution network was created with 10-node element structure. The total number of nets used is 162139. The percentage of the item with an aspect ratio of less than 3 is 99.5%. Solid mesh is used as the mesh type. The real pin element is not used in the analysis model. This is to reduce the number of contacts and networks. The pin element has been defined by the program. Contact surfaces are defined between parts. No penetration contact type has been defined for these contact surfaces and the parts are prevented from intermingling. Since the reaction forces between the contact surfaces are an important factor for the stress values that will occur in the finger model, this contact definition has been made.

## 3. Results and Discussion

In the study, a single degree of freedom rotary connection type defined as P5 was used for finger connections by reducing the finger movement to planar dimension. The prosthetic hand and movement functions produced were given in Figures 7 and 8.

Thus, kinematic and dynamic analyzes of the fingers were made under different boundary conditions. The torque values calculated according to the angles and forces of the index finger were shown in Table 7.

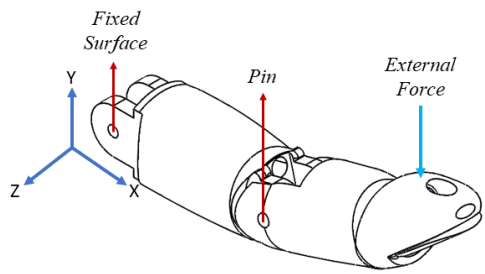


Figure 6. Boundary conditions applied for static analysis

Figure 7. Images of the produced prosthetic hand in the open position

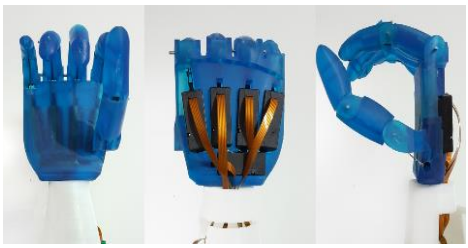

Figure 8. Images of produced prosthetic hand in closed position

Table 7. Torque values calculated for index finger

| $\theta_1$ | $\theta_2$ | $\theta_3$ | $F_{dış}$ | $T_{total1}$ | $T_{total2}$ |
|---|---|---|---|---|---|
| 0º | 0º | 90º | 12,5N | 0,982Nm | 0,512Nm |
| 15º | 15º | 90º | 12,5N | 0,966Nm | 0,508Nm |
| 30º | 30º | 90º | 12,5N | 0,919Nm | 0,496Nm |
| 45º | 45º | 90º | 12,5N | 0,844Nm | 0,476Nm |
| 60º | 60º | 90º | 12,5N | 0,747Nm | 0,449Nm |
| 75º | 75º | 90º | 12,5N | 0,634Nm | 0,416Nm |
| 90º | 90º | 90º | 12,5N | 0,512Nm | 0,377Nm |

Torque values calculated according to angles and forces of the middle finger was shown in Table 8. Torque values calculated according to angles and forces of the ring finger was shown in Table 9. Torque values calculated according to angles and forces of the little finger was shown in Table 10.

The torque forces to the MCP and PIP joints are graphically explained in Figure 9. Maximum torque values were obtained at the middle finger. Minimum torque values were observed on the little finger. The torque values of index and ring fingers were close to each other for all boundary conditions.

Table 8. Torque values calculated for middle finger

| $\theta_1$ | $\theta_2$ | $\theta_3$ | $F_{dış}$ | $T_{total1}$ | $T_{total2}$ |
|---|---|---|---|---|---|
| 0º | 0 | 90º | 17,5N | 1,564Nm | 0,820Nm |
| 15º | 15º | 90º | 17,5N | 1,538Nm | 0,814Nm |
| 30º | 30º | 90º | 17,5N | 1,464Nm | 0,795Nm |
| 45º | 45º | 90º | 17,5N | 1,346Nm | 0,764Nm |
| 60º | 60º | 90º | 17,5N | 1,191Nm | 0,721Nm |
| 75º | 75º | 90º | 17,5N | 1,012Nm | 0,669Nm |
| 90º | 90º | 90º | 17,5N | 0,820Nm | 0,607Nm |

Table 9. Torque values calculated for the ring finger

| $\theta_1$ | $\theta_2$ | $\theta_3$ | $F_{dış}$ | $T_{total1}$ | $T_{total2}$ |
|---|---|---|---|---|---|
| 0º | 0 | 90º | 12,5N | 1,004Nm | 0,510Nm |
| 15º | 15º | 90º | 12,5N | 0,987Nm | 0,506Nm |
| 30º | 30º | 90º | 12,5N | 0,938Nm | 0,483Nm |
| 45º | 45º | 90º | 12,5N | 0,859Nm | 0,472Nm |
| 60º | 60º | 90º | 12,5N | 0,757Nm | 0,444Nm |
| 75º | 75º | 90º | 12,5N | 0,638Nm | 0,408Nm |
| 90º | 90º | 90º | 12,5N | 0,510Nm | 0,366Nm |

Table 10. Torque values calculated for the little finger

| $\theta_1$ | $\theta_2$ | $\theta_3$ | $F_{dış}$ | $T_{total1}$ | $T_{total2}$ |
|---|---|---|---|---|---|
| 0º | 0 | 90º | 7,5N | 0,522Nm | 0,268Nm |
| 15º | 15º | 90º | 7,5N | 0,513Nm | 0,266Nm |
| 30º | 30º | 90º | 7,5N | 0,488Nm | 0,260Nm |
| 45º | 45º | 90º | 7,5N | 0,448Nm | 0,249Nm |
| 60º | 60º | 90º | 7,5N | 0,395Nm | 0,235Nm |
| 75º | 75º | 90º | 7,5N | 0,331Nm | 0,217Nm |
| 90º | 90º | 90º | 7,5N | 0,268Nm | 0,195Nm |

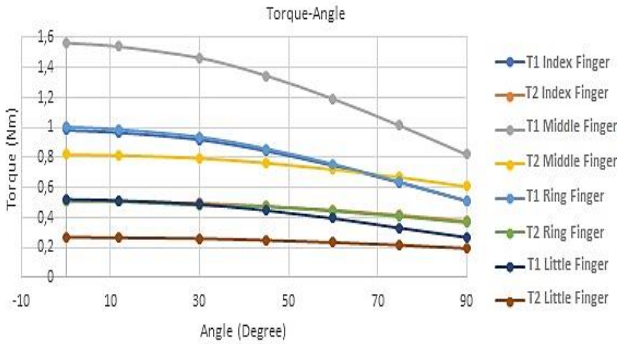


Figure 9. T1 and T2 graphics according to the position angles of the fingers

In the static analysis of the study, the maximum stress values were obtained in the joint region according to the vonmisses error criteria and the results are shown in Figures 10, 11, 12, 13, 14, 15 and 16, respectively.

As seen in Figure 17, this value in the joint region ranges from 35 MPa to 18 MPa. These values are the nodal stress values.

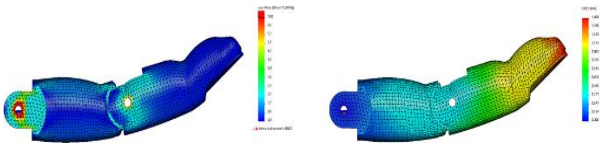

Figure 10. Stress and displacement graph for θ_1= 0º and θ_2= 0º configurations

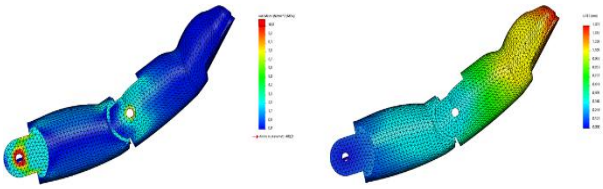

Figure 11. Stress and displacement graph for θ_1= 15º and θ_2= 15º configurations

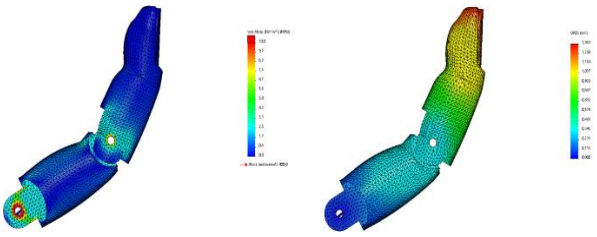

Figure 12. Stress and displacement graph for θ_1= 30º and θ_2= 30º configurations

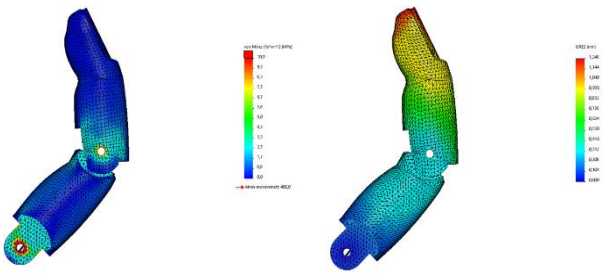

Figure 13. Stress and displacement graph for θ_1= 45º and θ_2= 45º configurations

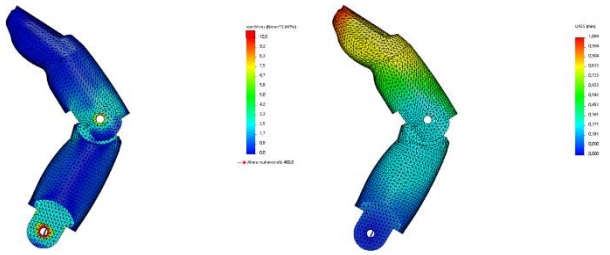

Figure 14. Stress and displacement graph for θ_1= 60º and θ_2= 60º configurations

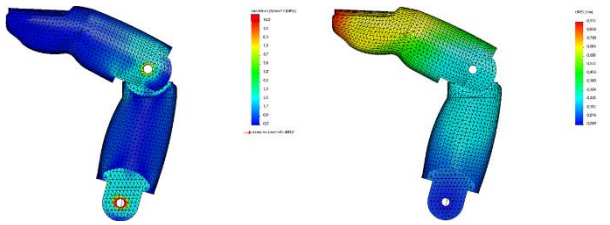

Figure 15. Stress and displacement graph for θ_1= 75º and θ_2= 75º configurations

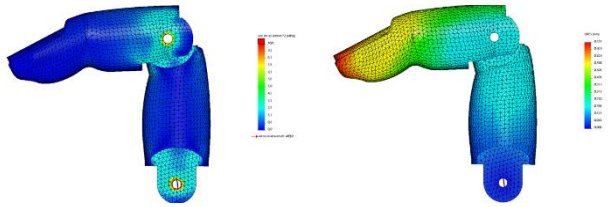

Figure 16. Stress and displacement graph for θ_1= 90º and θ_2= 90º configurations

Figure 17. Stress graph according to the position angles of the index finger

The displacement values were calculated between 1.473 mm and 0.751. The graphic of the displacement of the index finger relative to the angle of change specified in the range of Figures 8 and 14 was shown in Figure 18.

Figure 18. Displacement graph according to the position angles of the index finger

Special silicone hands were prepared to have a realistic appearance after 3D scanning and editing. Human skin color, hair and nail details were taken into consideration in the production of silicone covers. When the products on the market were examined, there are two types of silicone sleeves. The first of these is the silicone used in prosthetic hands. Silicone hands were passed over the prosthesis, both closing the mechanical image of the prosthesis and creating a realistic image by working with it. The second is passive silicone hand coating. They were used only for display purposes and the wall thickness is quite high. In this study, both silicone hands were studied in the prosthesis. Both silicone hands can be used on the go, as the design is unique. However, the project continued with other silicone gloves, as it was seen that the motors consume too much power for passive silicone gloves with high wall thickness.

## 4. Conclusion

The prosthetic hand was produced and assembled on a 3D printer using clear resin. The production took about 7 hours, and the production and quality control of the whole process was provided for around 20 hours together with the assembly and trials. Production was made with extremely low costs in terms of cost. As shown in Figures 7 and 8, the prosthetic hand was tested on an amputated person using a silicon sheath. Glass holding position was studied during the trial. Finger speed settings were calibrated in the trials, and thumb movement was provided manually by the person. As a result of the trials, the hand held the glass normally and let it go. This prosthetic hand provided the amputee's cosmetic, appearance and control sensitivity that did not attract much attention in the society and positively affected the person.

In our future studies, we hope to do studies with electromyography or a completely neural network.

## Declaration

The author(s) declared no potential conflicts of interest with respect to the research, authorship, and/or publication of this article. The author(s) also declared that this article is original, was prepared in accordance with international publication and research ethics, and ethical committee permission or any special permission is not required.

## Author Contributions

M. Kayrıcı prepared experimental setup. Y. Uzun contributed to data collection phase and wrote the manuscript. O. Gök performed the analysis and mathematical modelling. H. Arıkan made proofreading of manuscript.

## Acknowledgment

This study was supported by the Scientific Research Projects Coordination Unit of Necmettin Erbakan University [Grant No: 161731002].

## References


1. Gürgül, S., Uzun, C., and Erdal, N., *Kemik biyomekaniği.* Gaziosmanpaşa Üniversitesi Tıp Fakültesi Dergisi, 2016. **8**(1): p. 18-34.
2. Naranjo, J., Miguel, C., Romero, M., and Saez L., *Structural numerical analysis of a three fingers prosthetic hand prototype.* International Journal of Physical Sciences, 2013. **8**(13): p. 526-536.
3. Clement, R.G., Bugler, K.E., and Oliver, C.W., *Bionic prosthetic hands: A review of present technology and future aspirations.* Surgeon, 2011. **9**(6): p. 336-340.
4. Pouliquen, M., Bernard, A., Marsot, J., and Chodorge, L., *Virtual Hands And Virtual Reality Multimodal Platform To Design Safer Industrial Systems.* Computers in Industry, 2007. **58**(1): p. 46-56.
5. Kerpa, O., Osswald, D., Yigit, S., Burghart, C., and Woern, H., *Arm-hand control by tactile sensing for human robot co-operation.* Proc.Humanoids'2003, **1**(1): p. 1-12.
6. Butz, K.D., Merrell, G., and Nauman, E.A., *A biomechanical analysis of finger joint forces and stresses developed during common daily activities.* Computer Methods in Biomechanics and Biomedical Engineering, 2012. **15**(2): p. 131-140.
7. Dechev, N., Cleghorn,W.L., and Naumann, S., *Multiple finger, passive adaptive grasp prosthetic hand.* Mechanism and Machine Theory, 2001. **36**(10): p. 1157-1173.
8. El Kady, A.M., Mahfouz, A.E., and Taher, M.F., *Mechanical design of an anthropomorphic prosthetic hand for shape memory alloy actuation.* In: 2010 5th Cairo International Biomedical Engineering Conference, CIBEC 2010, 2010. p. 1157-1173.
9. Kuran, B., *El rehabilitasyonu*. 1995, Nobel Tıp Kitapları.
10. Durand, R., Pantoja-Rosero, B., and Oliveria, V., *A general mesh smoothing method for finite elements*. Finite Elements in Analysis and Design, 2019. **158**(1): p. 17-30.
11. Weightman, B., and Amis, A.A., *Finger joint force predictions related to design of joint replacements.* J Biomed Eng., 1982. **4**(3): p. 197-205
12. Atasoy, A., Kuchimov, S., Toptas, E., Kaplanoglu, E., Takka, S., and Ozkan, M., *Finger design for anthropomorphic prosthetic hands.* 2014 18th National Biomedical Engineering Meeting, BIYOMUT 2014, 2015. p. 1-3.
13. Özkan, S.S., Karayel, D., Atalı, G., and Gökbayrak, I., *Esnek Algılayıcı Kontrollü Robot El Tasarımı ve Gerçeklenmesi.* Academic Platform Journal of Engineering and Science, 2017. p. 35-40.
14. Carozza, M.C., Cappiello, G., Stellin, G., Zaccone, F., Vecchi, F., Micera, S., and Dario, P., *On the development of a novel adaptive prosthetic hand with compliant joints: experimental platform and emg control.* 2005 IEEE/RSJ International Conference on Intelligent Robots and Systems, 2005. p. 1271-1276.
15. Anatomical hand structure. [cited 2020 29 Nov]; Available from:*http://pulpbits.net/4-human-skeleton-hand-diagrams/animation-of-skeleton-hands.*
16. Lin, J.,Wu, Y., and Huang, T.S., *Modeling the constraints of human hand motion.* Proceedings, Workshop on Human Motion, HUMO, 2000. **7**(2): p. 121-126.
17. Cobos, S., Ferre, M.and Sanchéz-Urán, M.A., Ortego, J., and Peña, C., *Efficient human hand kinematics for manipulation tasks.* In: 2008 IEEE/RSJ International Conference on Intelligent Robots and Systems, IROS, 2008. **8**(3): p. 2246-2251.
18. Ryew, S., and Choi, H., *Double active universal joint (dauj): Robotic joint mechanism for humanlike motions.* IEEE Transactions on Robotics and Automation, 2001. **17**(2): p. 290-300.
19. Xu, Z., and Todorov, E., *Design of a highly biomimetic anthropomorphic robotic hand towards artificial limb regeneration.* Proceedings - IEEE International Conference on Robotics and Automation, 2016. **12**(2): p. 3485-3492.
20. Joseacute, A.L.N., Christopher, R.T.S.M., Manuel, F.C.R., and Ez Luis, M.N.S., *Structural numerical analysis of a three fingers prosthetic hand prototype.* International Journal of Physical Sciences, 2013. **8**(3): p. 526-536.
21. Harih, G., Tada, M., and Dolšak, B., *Justification for a 2d versus 3d fingertip finite element model during static contact simulations.* Computer Methods in Biomechanics and Biomedical Engineering, 2016. **19**(3): p. 1409-1417.
22. Antoanela, N., Ardelean, D., and Srl, T., *The application of the finite element method in the biomechanics of the human upper limb and of some prosthetic components.* WSEAS Transactions on Computers, 2009. **8**(2): p. 1296-1305.
23. Gray, H., Warwick, R., and Williams, P.L., *Gray's Anatomy.* 1973, 35 ed., Longman.
24. Kouchi, M., and Tada, M., *Digital Hand: Interface Between the Robot Hand and Human Hand.* Human Inspried Dexterity in Robotic Manupilation, Academic Press, 2018. **11**(3): p. 11-26.
25. Vishwakarma, P., and Sharma, A., *3d finite element analysis of milling process for non-ferrous metal using deform-3d*. Materials Today, Proceedings, 2019. **26**(2): p. 2726-2733.
26. Anatomic finger structure. [cited 2020 29 Nov]; Available from: *https://en.wikipedia.org/wiki/Thumb*. Web. 29 Nov 2020.

## Appendix

$$ {}^{i-1}_{i}T = \begin{bmatrix} \cos\theta_i & -\sin\theta_i & 0 & a_{i-1} \\ \sin\theta_i \cos\alpha_{i-1} & \cos\theta_i \cos\alpha_{i-1} & -\sin\alpha_{i-1} & -\sin\alpha_{i-1}\, d_1 \\ \sin\theta_i \sin\alpha_{i-1} & \cos\theta_i \sin\alpha_{i-1} & \cos\alpha_{i-1} & \cos\alpha_{i-1}\, d_i \\ 0 & 0 & 0 & 1 \end{bmatrix} \tag{A1} $$

For the 1st joint, *(i=1)*, ${}^{i-1}_{i}T = {}^{1-1}_{1}T = {}^{0}_{1}T$

$$ {}^{0}_{1}T = \begin{bmatrix} \cos\theta_1 & -\sin\theta_1 & 0 & a_0 \\ \sin\theta_1 \cos\alpha_0 & \cos\theta_1 \sin\alpha_0 & -\sin\alpha_0 & -\sin\alpha_0\, d_1 \\ \sin\theta_1 \sin\alpha_0 & \cos\theta_1 \sin\alpha_0 & \cos\alpha_{1-1} & \cos\alpha_0\, d_1 \\ 0 & 0 & 0 & 1 \end{bmatrix} = \begin{bmatrix} \cos\theta_1 & -\sin\theta_1 & 0 & 0 \\ \sin\theta_1 & \cos\theta_1 & 0 & 0 \\ 0 & 0 & 1 & 0 \\ 0 & 0 & 0 & 1 \end{bmatrix} \tag{A2} $$

For the 2nd joint, *(i=2)*, ${}^{i-1}_{i}T = {}^{2-1}_{2}T = {}^{1}_{2}T$ ,

$$ {}^{1}_{2}T = \begin{bmatrix} \cos\theta_2 & -\sin\theta_2 & 0 & a_{2-1} \\ \sin\theta_2 \cos\alpha_{2-1} & \cos\theta_2 \cos\alpha_{2-1} & -\sin\alpha_{2-1} & -\sin\alpha_{2-1}\, d_2 \\ \sin\theta_2 \sin\alpha_{2-1} & \cos\theta_2 \cos\alpha_{2-1} & \cos\alpha_{2-1} & \cos\alpha_{2-1}\, d_2 \\ 0 & 0 & 0 & 1 \end{bmatrix} = \begin{bmatrix} \cos\theta_2 & -\sin\theta_2 & 0 & l_1 \\ \sin\theta_2 & \cos\theta_2 & 0 & 0 \\ 0 & 0 & 1 & 0 \\ 0 & 0 & 0 & 1 \end{bmatrix} \tag{A3} $$

For the 3rd joint, *(i=3)*, ${}^{i-1}_{i}T = {}^{3-1}_{3}T = {}^{2}_{3}T$

$$ {}^{2}_{3}T = \begin{bmatrix} \cos\theta_3 & -\sin\theta_3 & 0 & a_{3-1} \\ \sin\theta_3 \cos\alpha_{3-1} & \cos\theta_3 \sin\alpha_3 & -\sin\alpha_{3-1} & -\sin\alpha_{3-1}\, d_3 \\ \sin\theta_3 \sin\alpha_{3-1} & \cos\theta_3 \sin\alpha_3 & \cos\alpha_{3-1} & \cos\alpha_{3-1}\, d_3 \\ 0 & 0 & 0 & 1 \end{bmatrix} = \begin{bmatrix} 1 & 0 & 0 & l_2 \\ 0 & 1 & 0 & 0 \\ 0 & 0 & 1 & 0 \\ 0 & 0 & 0 & 1 \end{bmatrix} $$

$$ {}^{0}_{3}T = {}^{0}_{1}T\,{}^{1}_{2}T\,{}^{2}_{3}T $$

$$ {}^{0}_{3}T = \begin{bmatrix} \cos\theta_1 & -\sin\theta_1 & 0 & 0 \\ \sin\theta_1 & \cos\theta_1 & 0 & 0 \\ 0 & 0 & 1 & 0 \\ 0 & 0 & 0 & 1 \end{bmatrix} \begin{bmatrix} \cos\theta_2 & -\sin\theta_2 & 0 & l_1 \\ \sin\theta_2 & \cos\theta_2 & 0 & 0 \\ 0 & 0 & 1 & 0 \\ 0 & 0 & 0 & 1 \end{bmatrix} \begin{bmatrix} 1 & 0 & 0 & l_2 \\ 0 & 1 & 0 & 0 \\ 0 & 0 & 1 & 0 \\ 0 & 0 & 0 & 1 \end{bmatrix} $$

$$ {}^{0}_{3}T = \begin{bmatrix} \cos\theta_{12} & -\sin\theta_{12} & 0 & l_1 \cos\theta_1 + l_2 \cos\theta_{12} \\ \sin\theta_{12} & \cos\theta_{12} & 0 & l_1 \sin\theta_1 + l_2 \sin\theta_{12} \\ 0 & 0 & 1 & 0 \\ 0 & 0 & 0 & 1 \end{bmatrix} \tag{A4} $$

*Kinetic energy;*

$$ S = S_1 + S_2 = \frac{1}{2} m_1 \left(\dot{x}_1{}^2 + \dot{y}_1{}^2\right) + \frac{1}{2} m_2 \left(\dot{x}_2{}^2 + \dot{y}_2{}^2\right) $$

$$ = \frac{1}{8} m_1 l_1{}^2 \dot{\theta}_1{}^2 + \frac{1}{2} m_2 \left[ l_1{}^2 \dot{\theta}_1{}^2 + \frac{l_2{}^2}{4} (\dot{\theta}_1 + \dot{\theta}_2)^2 + l_1 l_2 \cos\theta_1\, \dot{\theta}_1 \left(\dot{\theta}_1 + \dot{\theta}_2\right) \left(l_1 l_2 \cos\theta_1\, \dot{\theta}_1 \left(\dot{\theta}_1 + \dot{\theta}_2\right) \cos(\theta_1 + \theta_2)\right) \right] \tag{A5} $$

*Potential energy;*

$$ V = V_1 + V_2 = m_1 g Y_1 + m_2 g Y_2 = m_1 g \frac{l_1}{2} \sin\theta_1 + m_2 g \left[ (l_1 \sin\theta_1 + \frac{l_2}{2} \sin(\theta_1 + \theta_2) \right] \tag{A6} $$

*L=S-V*

$$ = \frac{1}{8} m_1 l_1{}^2 \dot{\theta}_1{}^2 + \frac{1}{2} m_2 \left[ l_1{}^2 \dot{\theta}_1{}^2 + \frac{l_2{}^2}{4} (\dot{\theta}_1 + \dot{\theta}_2)^2 + l_1 l_2 \cos\theta_1\, \dot{\theta}_1 \left(\dot{\theta}_1 + \dot{\theta}_2\right) \left(l_1 l_2 \cos\theta_1\, \dot{\theta}_1 \left(\dot{\theta}_1 + \dot{\theta}_2\right) \cos(\theta_1 + \theta_2)\right) \right] - m_1 g \frac{l_1}{2} \sin\theta_1 + m_2 g \left[ (l_1 \sin\theta_1 + \frac{l_2}{2} \sin(\theta_1 + \theta_2) \right] \tag{A7} $$

$$ \left(\frac{\partial L}{\partial \theta_1}\right) = -\left(\frac{m_1}{2} + m_2\right) g l_1 \cos\theta_1 - m_2 g \frac{l_2}{2} \cos(\theta_1 + \theta_2) $$

$$ \frac{\partial L}{\partial \dot{\theta}_1} = (\frac{m_1}{4} + m_2)\, l_1{}^2 \dot{\theta}_1 + \frac{l_2}{4} m_2 l_2{}^2 \left(\dot{\theta}_1 + \dot{\theta}_2\right) + \frac{1}{2} m_2 l_1 l_2 (2\dot{\theta}_1 + \dot{\theta}_2) \cos\theta_2 $$

$$ \frac{d}{dt}\left(\frac{\partial L}{\partial \dot{\theta}_1}\right) = \left(\frac{m_1}{4} + m_2\right) l_1{}^2 \ddot{\theta}_1 + \frac{1}{4} m_2 l_2{}^2 \left(\ddot{\theta}_1 + \ddot{\theta}_2\right) + \frac{1}{2} m_2 l_1 l_2 \left(2\ddot{\theta}_1 + \ddot{\theta}_2\right) \cos\theta_2 - \frac{1}{2} m_2 l_1 l_2 \dot{\theta}_2 (2\dot{\theta}_1 + \dot{\theta}_2) \sin\theta_2 \tag{A8} $$

$$\left(\frac{\partial L}{\partial \theta_2}\right) = -\frac{1}{2} m_2 l_1 l_2 \dot{\theta}_1 (\dot{\theta}_1 + \dot{\theta}_2) sin\theta_2 - m_2 g \frac{l_2}{2} cos\,(\theta_1 + \theta_2)$$

$$\left(\frac{\partial L}{\partial \dot{\theta}_2}\right) = \frac{1}{4} m_2 {l_2}^2 (\dot{\theta}_1 + \dot{\theta}_2) + \frac{1}{2} m_2 l_1 l_2 \dot{\theta}_1\, cos\theta_2$$

$$\frac{d}{dt}\left(\frac{\partial L}{\partial \dot{\theta}_2}\right) = \frac{1}{4} m_2 {l_2}^2 (\ddot{\theta}_1 + \ddot{\theta}_2) + \frac{1}{2} m_2 l_1 l_2 \ddot{\theta}_1\, cos\theta_2 - \frac{1}{2} m_2 l_1 l_2 \dot{\theta}_1 \dot{\theta}_2\, sin\theta_2$$

$$T_{internal1} = \frac{d}{dt}\left(\frac{\partial L}{\partial \dot{\theta}_1}\right) - \left(\frac{\partial L}{\partial \theta_1}\right)$$

$$= \left(\frac{m_1}{4} + m_2\right) {l_1}^2 \ddot{\theta}_1 + \frac{1}{4} m_2 {l_2}^2 (\ddot{\theta}_1 + \ddot{\theta}_2) + \frac{1}{2} m_2 l_1 l_2 (2\ddot{\theta}_1 + \ddot{\theta}_2)\, cos\theta_2 - \frac{1}{2} m_2 l_1 l_2 \dot{\theta}_2 (2\dot{\theta}_1 + \dot{\theta}_2) sin\theta_2 +$$

$$\left(\frac{m_1}{2} + m_2\right) g l_1\, cos\,\theta_1 + m_2 g \frac{l_2}{2} cos\,(\theta_1 + \theta_2)$$

$$T_{internal\,2} = \frac{d}{dt}\left(\frac{\partial L}{\partial \dot{\theta}_2}\right) - \left(\frac{\partial L}{\partial \theta_2}\right)$$

$$= m_2 \frac{{l_2}^2}{4} (\ddot{\theta}_1 + \ddot{\theta}_2) + \frac{1}{2} m_2 l_1 l_2 \ddot{\theta}_1\, cos\theta_2 - \frac{1}{2} m_2 l_1 l_2 \dot{\theta}_1 \dot{\theta}_2\, sin\theta_2 + \frac{1}{2} m_2 l_1 l_2 \dot{\theta}_1 (\dot{\theta}_1 + \dot{\theta}_2)\, sin\theta_2 + \tag{A9}$$

$$m_2 g \frac{l_2}{2} cos\,(\theta_1 + \theta_2)$$

$$\begin{bmatrix} T_{total1} \\ T_{total2} \end{bmatrix} = \begin{bmatrix} T_{internal1} \\ T_{internal2} \end{bmatrix} + \begin{bmatrix} F_{external1} \\ F_{external2} \end{bmatrix} \begin{bmatrix} Pxy1 \\ Pxy2 \end{bmatrix} \tag{A10}$$